Early Damage Detection in Epoxy Matrix Using Cyclobutane-based Polymers

Jin Zou, Yingtao Liu, Bohan Shan, Aditi Chattopadhyay and Lenore L. Dai*

School for Engineering of Matter, Transport, and Energy

Arizona State University, Tempe, AZ 85287

*Corresponding author: 480-965-4112; Lenore.Dai@asu.edu

Abstract

Identification of early damage in polymer composites is of great importance. We have incorporated cyclobutane-containing crosslinked polymers into an epoxy matrix, studied the effect on thermal and mechanical properties and more importantly, demonstrated early damage detection through mechanically induced fluorescence generation. Two cinnamate derivatives, 1,1,1-tris(cinnamoyloxymethyl) ethane (TCE) and poly(vinyl cinnamate) (PVCi), were photoirradiated to produce cyclobutane-containing polymer, respectively. The effects on the thermal properties and mechanical properties with the addition of cyclobutane-containing polymer into epoxy matrix were investigated. The emergence of cracks was detected by fluorescence at a strain level right beyond the yield point of the polymer blends and the fluorescence intensified with accumulation of strain. Overall, the results show that the damages can be detected through fluorescence generation along the crack propagation.

Keywords: cinnamate; cyclobutane; epoxy; stress-strain; crack sensor

1. INTRODUCTION

Material degradation, caused by mechanical deformation, thermal expansion/contraction, radioactive contamination, chemical corrosion or electrical discharges, occurs inevitably in practical applications and significantly reduces material performance, especially in harsh environments [1-4]. For example, aerospace materials are exposed to large changes in pressure, temperature, speed and other elements. All these elements can cause large accumulations of stresses on the materials [5]. Beyond a certain threshold, microscopic cracks will begin to form and grow irreversibly, which eventually result in complete destruction of the materials and jeopardize public safety [6-8]. It is of great importance to monitor the health conditions of materials in service; therefore people can take steps before materials reach mechanic failure.

Scientists study many years to develop the damage detection technology. Recent research has shown that the utilization of electro-mechanical (E/M) impedance methods allow for the direct identification of structural dynamics [9-11]. The mechanism is to couple small-size piezoelectric active sensors, like lead zirconate titanate, with the material structure. The measurements of the E/M impedance or admittance signatures are related to the mechanical impedance which is affected by the presence of damage. Lamb wave method is also suitable for structural health monitoring applications [12-13].

Damage in a structure can be also by identified by a self-monitoring material, like crack sensors. Several types of crack sensors have been developed in the recent years [14-16]. Especially, due to ease of detection, many efforts have been devoted to develop methods of detecting damage in terms of visibility. A visible color change can indicate areas under stress and offer a signal if there is damage occurred. Mechanofluorochromic materials which depend on changes

in physical molecular packing modes in responsive to mechanical stimuli can be used as stress sensors [17-19]. Crenshaw et al., as pioneers in organic mechanofluorochromism, demonstrated that tensile deformation could facilitate substantial changes in the luminescent properties of linear low-density polyethylene (LLDPE)–dye blends by the destruction of dye aggregates [19]. The deformation color can be tuned by varying the electronics molecular structures of the dye molecules. However, the limited solubility of the organic dye in the polymer matrix limits the application of this system in some materials. Materials that respond to external stress with a color change are already known, but most of the color change processes are activated by the disruption or formation of non-covalent bonds. Mechanophore, a force sensitive unit, gives visible color change upon the scission of covalent bonds on structure. In recent years, mechanophore-linked polymers have attracted significant interest, since this expands the scope of applications by allowing a variety of polymers to be accessed. Sijbesma et al. synthesized stress-sensitive polymer by incorporating the bis(adamantly)-1,2-dioxetanes unit which enabled transduction of force into a temporal visible luminescence under stress by opening of the four-membered dioxetane ring with subsequent ketone product relaxation from its excited state to the ground state [20]. Pyran-based organic compounds, like spiropyrans, spirooxazines, naphthopyrans, are well known chromogenic materials of which structure changes occur in company with a color change induced by temperature or light [21-24]. However, color change induced by external force in pyran-based compounds is not well reported. Davis et al. synthesized spiropyran-linked elastomeric polymers which could act as a force sensor in response to the stress loading [25]; this response was accompanied by a color change through a mechanically induced 6-electrocyclic ring-opening reaction from colorless spiropyran to colored merocyanine conformations.

Although mechanophore-linked polymer has opened tremendous new opportunities, especially in the areas of stress-sensing and crack/failure early detection, there remain many unknown fundamentals as well as unexplored applications. The current research emphasizes more on pure and bulk traditional polymers; the synthesis solely relies on individual chemistry/reaction mechanism which is often limited and complicated. Here we designed and synthesized a mechanically responsive composite material system by blending the cyclobutane-containing polymer into an epoxy matrix to identify the damage location through mechanically induced fluorescence generation.

2. METHODOLOGY

Materials

Unless otherwise stated, all the materials and reagents listed below were used as received. 1,1,1-tris(hydroxymethyl)ethane (99%), cinnamoyl chloride (98%), tetrahydrofuran (≥99.9%), 4-(dimethylamino)pyridine (≥99%),dichloromethane (≥99.8%), ethanol (≥99.5%) and poly(vinyl cinnamate) (PVCi, average M_n 45,000-55,000) were purchased from Sigma-Aldrich. Sodium chloride (≥99%) and water (HPLC) were purchase from Fisher Scientific. Epoxy resin FS-A23 (digycidylether of bisphenol F, DGEBPF) and epoxy hardener FS-B412 (diethylenetriamine, DETA) were purchased from Epoxy System Inc.

Synthesis of 1,1,1- tris (cinnamoyloxymethyl) ethane (TCE)

TCE was prepared through the reaction between 1,1,1-tris(hydroxymethyl)ethane and cinnamoyl chloride [26]. The crude product was purified by recrystallization through hot ethanol. [1]H and ^{13}C nuclear magnetic resonance (NMR) spectra were taken on Bruker 400 MHz NMR

spectrometer. The ^{1}H NMR (CDCl$_3$) data for TCE are as follow: δ1.178 (s, 3H, CH$_3$), 4.292 (s, 6H, OCH$_2$), 6.442 (d, 3H, J = 16 Hz, phCH), 7.260-7.504 (m, 15H, phenyl), 7.688 (d, 3H, J = 16 Hz, phCH), ^{13}C NMR (CDCl$_3$): δ17.402 (CH$_3$), 38.839 (CCH$_3$), 66.282 (OCH$_2$), 117.544, 128.173, 128.895, 134.209 (phenyl), 130.435 (phCH), 145.411 (phCH=CH), 166.699 (carbonyl). Mass spectra were conducted on JEOL LCMate mass spectrometer. The calculated molecular mass for TCE is 511.2205 and [M-H] at 510.2042 was detected experimentally.

Preparation of cyclobutane-containing polymer and polymer blends

To prepare TCE polymer or PVCi polymer, TCE or PVCi solid was dissolved in CH$_2$Cl$_2$ first. The solution was applied on a clean silicon mold to form a thin film and placed in vacuum to evaporate the excess CH$_2$Cl$_2$. After the evaporation of CH$_2$Cl$_2$, the thin film was photoirradiated at 302 nm for 4 hr. All the silicon molds and glass slides for preparation of samples were used with pretreatment with mold release agent.

To prepare polymer/epoxy polymer blends, the TCE or PVCi solution was added to DGEBPF and dispersed well using an ultrasonic probe sonicator (Sonics VibraCell, 500 W model). The mixture was placed in a vacuum chamber at 50 °C to evaporate the CH$_2$Cl$_2$ until the mass of the mixture kept unchanged, indicating the excess CH$_2$Cl$_2$ was evaporated. The resin mixture was cooled down to room temperature before DETA was added and mixed (M$_{TCE}$ or $_{PVCi}$: M$_{Epoxy}$=1:10; M$_{DGEBPF}$: M$_{DETA}$= 100:27). The mixture was sonicated in ice bath to prevent any premature curing. After the mixture became homogenous, the mixture was poured into the silicon molds and moved into a vacuum chamber to degas for 30 minutes, followed by photoirradiation conducted by an UV lamp with 302 nm wavelength (UVP, UVM-28). According to the manufacturer's data, the light density is approximately 1300 μW/cm^2 at a

distance of 3 cm. The sample was exposed to UV for 4 hr and cured overnight at room temperature in atmosphere. Neat epoxy sample followed the similar procedure for comparison. After simple machining, the sample was ready for test. The average dimension of cubic sample was 3×4×8 mm.

Characterization of photochemical properties of cinnamates

All UV spectroscopic analyses were performed on a UV-Vis spectrometer (Perkin Elmer Lambda 18). The spectra of the samples were recorded before exposure and after each exposure at selected intervals of time. All measurements were performed using same parameters at room temperature. The FT-IR spectra were analyzed on Bruker IFS 66V/S FTIR spectrometer. TCE was dissolved in CH_2Cl_2 and was spread out on KBr disk and left without any disturbance. CH_2Cl_2 was then evaporated off in a vacuum oven at room temperature to form a very thin film.

Characterization of polymer blends

The measurements of T_g were carried out with differential scanning calorimeter thermal analysis (DSC). The experiments were performed in a nitrogen atmosphere using TA Instruments Q20. Throughout the DSC work, temperature and heat flow calibrations were performed following standardized procedures. After a heating and cooling cycle up to 70 °C with a heating ramp rate of 10 °C /min to eliminate the thermal history, T_g was analyzed from the data of the second heating scan from -20 to 120 °C at 10 °C/min, with the TA Universal Analysis software. All samples were contained in tzero pans with lids. An empty pan with a lid was used as reference. Thermogravimetric analysis (TGA) was carried out using a TA Instruments (TGA Q500 machine). The sample was placed in a tared platinum crucible. All the samples were heated from 30 to 600 °C at a heating rate of 10 °C/min in nitrogen. The compressive stress-strain curves of these systems were obtained by conducting on MTS servo hydraulic test system.

Tests were run in displacement control in longitudinal direction at loading rate of 1 mm/min. The samples were compressed to different strains. To monitor the fluorescence generation from cracked polymer blends, the cubic samples of polymer blends were compressed to different strains and observed simultaneously under the fluorescence microscope (Nikon Elipse TE300 inverted video microscope) by exposure to 330-380 nm UV light.

3. RESULTS AND DISCUSSION

Photoreaction of TCE and PVCi

In our study, we applied epoxy as the matrix materials. Epoxies are among the most popular thermosetting polymers and widely used in automobiles, aircraft, sports equipment and other areas due to their excellent mechanical performance, thermal stability and flame retardancy [27-30]. Cyclobutane was applied into the epoxy as mechanophores: 1,1,1-tris(cinnamoyloxymethyl) ethane (TCE) was dimerized through [2+2] cycloadddtion into cyclobutane ring under photoirradiation to eventually form a three-dimensional network. This cyclic product has been proved to efficiently generate fluorescence emission upon the cleavage of the cyclobutane ring [31]. The [2+2] photocycloadditon of the cinnamoyl groups was analyzed using both UV-Vis and FTIR spectroscopy. Figure 1(a) displays the UV absorbance variation of TCE dilute solution as a function of UV exposure time. It had strong UV absorbance between 250 and 350 nm with a peak centered at approximately 280 nm; this likely corresponds to the abundance of π-π* transitions of the C=C double bond from cinnamoyl groups before photoirradiation, as reported elsewhere [26, 32-33]. The change in the absorbance value was monitored for continual irradiation, and it is obvious to notice that the absorbance band decreases rapidly with exposure time and disappears almost completely within 30 minutes of photoirradiation. The observation implies the

7

formation of cyclobutane. The spectra had a slight blue shift from 280 to 272 nm due to the change in chemical structure of cinnamate groups under photoirradiation. For comparison, we also purchased PVCi which has the cinnamate functional group as side groups of the polymer chain to produce cyclobutane upon photoirradiation. PVCi is very prominent in photochemistry with some attractive characteristics [34-36]. The UV absorbance of PVCi dilute solution had a similar trend with TCE solution upon photoirradiation, as displayed in Figure 1 (b). The cycloaddition efficiency can be calculated according to the rate of disappearance of the C=C double bond of cinnamoyl group using the equation: conversion $(\%) = (A_0 - A_t)/A_0 \times 100$, where A_0 is the absorbance before irradiation at the maximal wavelength and A_t is the corresponding absorbance during photoreaction [37]. The conversion as a function of time is plotted in Figure 1 (inset) and estimated to be over 80% and 90% based on the absorbance change at 280 nm after 30 minutes of UV exposure. In addition, it was observed from both plots that conversion (%) never reached 100%. This can be explained by the steric hindrance from the formation of polymer network.
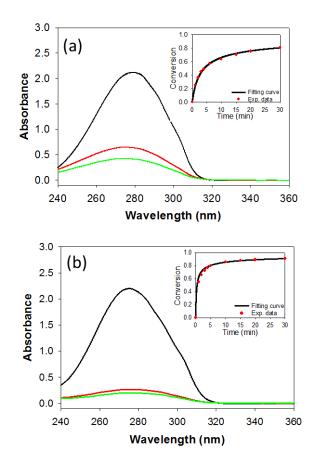
Figure 1. The change of UV absorbance of (a) TCE and (b) PVCi solution as UV exposure time (— 0 min; — 15min; — 30 min). The inset figures provide the change in the conversion as a function of the UV exposure time.

Results from FTIR were also used to track the functional groups transformation during photoirradiation. Figure 2 shows the FTIR spectra of TCE film before and after irradiation under UV light. The peaks at 1713 cm^{-1} and 1637 cm^{-1} corresponded to the conjugated C=O stretching vibration and vinylene C=C stretching vibration, as reported elsewhere [33, 38]. After 30 minutes of photoirradiation, the C=C peak disappeared due to consumption in forming cyclobutane by photo-dimerization, which destroyed the conjugation in the entire π-electron system. The C=O peak shifted to higher wavenumber with decreasing absorbance, this could be attributed to the loss of π–conjugation from C=C double bond [38-39].
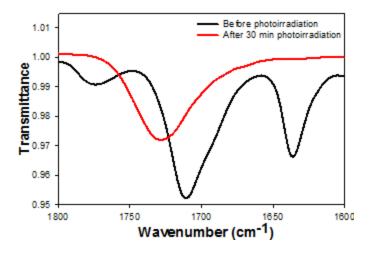
Figure 2. IR spectra of TCE film on a KBr disk before and after photoirradiation.

Effects of addition of polymers to the thermal and mechanical properties of polymer blends

Subsequently, we incorporated cyclobutane-containing polymers into an epoxy matrix and first studied glass transition temperatures (T_g).   Polymer blending was recognized as a very common way to develop new materials. Appropriate blending can offer extended useful properties compared to the neat ones. However, immiscibility and incompatibility are the main problems for most polymer blends which limit the usefulness in practical application. Fully miscible blends are characterized by a single glass transition temperature, unaffected by the number of polymer components the blends contain [40]. In contrast, immiscible blends for binary components usually have two glass transition temperatures. The DSC curves of   the neat epoxy and polymer blends are displayed in Figure 3. There is only one glass transition temperature observed for polymer blends, suggesting that the epoxy and cyclobutane-containing polymers were well miscible with each other. The miscibility of the blends was further confirmed by scanning electron microscope (SEM) in which no noticeable phase separation was detected.
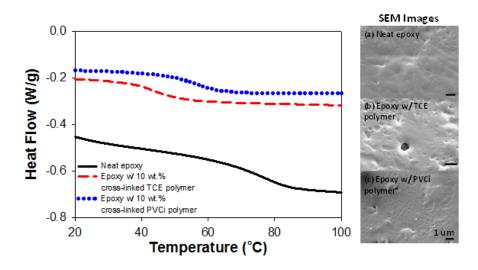
Figure 3. DSC curves and SEM images for neat epoxy and epoxy/polymer blends; (a) neat epoxy (b) epoxy with 10 wt. % TCE polymer (c) epoxy with 10 wt.% PVCi polymer.

It has been reported that T_g of epoxy polymer blends may vary due to different factors such as compositions of the blends or the conversion of the curing reaction [41-43]. The T_gs of the neat polymer and polymer blends are summarized in Table 1. The addition of TCE polymers or PVCi polymers to epoxy significantly changed the glass transition temperature. For a binary system, the T_g of the system can be calculated by the Fox equation: $\frac{1}{T_g} = \frac{x_1}{T_{g,1}} + \frac{1-x_1}{T_{g,2}}$, where $T_{g,i}$ is the glass transition temperature of component i, and x_i is the mass fraction of component i [40]. The comparisons between the experimental and theoretical values are shown in Figure 4. Theoretically, T_gs of epoxy with TCE polymers decease with the addition of TCE polymers and T_gs of epoxy with PVCi polymers increase with the addition of PVCi polymers, due to the lower T_g of TCE polymers and higher T_g of PVCi polymers than neat epoxy. Obviously, the measured values of samples were significantly deviated from the theoretical ones. Both experimental values decrease with the addition of contents of polymers and largely lower than the theoretical values. We hypothesize that the photo-cycloaddition of TCE or PVCi reduced the curing degree of epoxy significantly. The cross-linking reaction in neat epoxy was that the nucleophilic amine

on DETA attacked the carbon atom on ethylene oxide ring to form C-N bond [44]. TCE or PVCi introduced additional carbonyl group to the blends, which might influence the cross-linking process of epoxy due to the possible interactions between carbonyl group and amine. In addition, the low cross-linking of epoxy could be caused by the network formation by cycloaddition of cinnamates which restrained the motion and rotation of resin and hardener monomers during curing process. Therefore, the more additions of polymers will make the T_g much lower.
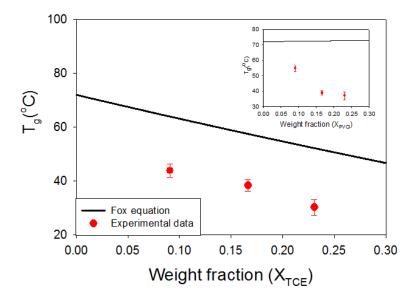

Figure 4. Comparisons of theoretical and experimental T_g of epoxy with various contents of TCE polymers and PVCi polymers (inset).

Table 1. T_g of polymer and polymer blends

	Neat epoxy	TCE polymer	PVCi polymer	Epoxy w/(10, 20, 30) wt.% TCE polymers	Epoxy w/(10, 20, 30) wt.% PVCi polymers
T_g, °C	72	0	75	44, 38, 29	55, 40, 36

Thermogravimetric analysis (TGA) was used for characterizing the thermal stability of the TCE polymers, PVCi polymers and polymer blends. Weight loss due to thermal degradation

is an irreversible process, which is highly related to oxidation through the interaction between the molecular bonds of a polymer and oxygen molecules [45-47]. Besides oxidation, polymers can be thermally degraded by random chain scission, side-group elimination and so on [48-49]. Since we run all the TGA measurements under nitrogen in our experiment, thermal degradation by oxidation was eliminated. The TGA and differential thermal gravimetry (DTG) curves as a function of temperature for TCE polymer and PVCi polymer are shown in Figure 5 (a). The peak of the DTG (T_p) indicated the point of greatest rate of change on the weight loss curve. Obviously, TCE polymer showed a higher initial decomposition temperature which started from 250 °C and completed at 430 °C. Thermal decomposition of PVCi polymer occurred at 100 °C. From DTG curve, TCE polymer had single major decomposition step; PVCi polymer had two subsequent major decomposition steps separated by a transition region, corresponding to the decomposition of cyclobutane and poly vinyl backbone [50].

TGA and DTG curves of neat epoxy and polymer blends are displayed in Figure 5 (b). Single step decomposition was observed in all the samples. The addition of TCE polymer or PVCi polymer increased the onset of thermal decomposition of epoxy slightly. From DTG curve, the value of derivative for epoxy with PVCi polymer was higher than epoxy and epoxy with TCE polymer. The T_p and the corresponding weight loss are summarized in Table 2. The data indicated that the addition of polymer increased the rate of degradation of epoxy, which could be attributed to the weaker cross-linking of epoxy.
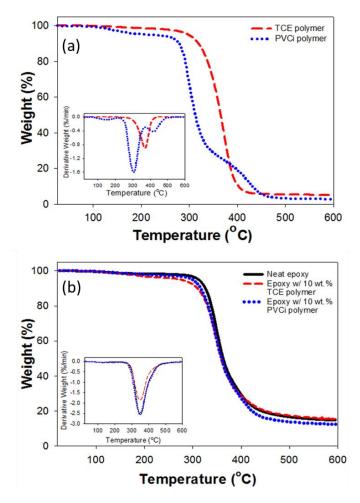
Figure 5. TGA and DTG curves (insets) of (a) TCE and PVCi polymers; (b) neat epoxy and polymer blends.

Table 2. T_p and the corresponding weight loss of polymer and polymer blends in TGA analysis

	Neat epoxy	TCE polymer	PVCi polymer	Epoxy w/10 wt.% TCE polymers	Epoxy w/10 wt.% PVCi polymers
T_p, °C	347	373	298 419	357	357
weight loss, %	31.1	61.4	30.4 86.3	47.9	47.9

Stress-strain curves of the neat epoxy and epoxy and polymer blends were determined in compression tests, as shown in Figure 6. The strain (%) is calculated from the ratio of displacement to the initial dimension. All these three systems displayed a qualitatively similar stress-strain behavior.   The curves exhibited an initial linear elastic response followed by yielding. With a slow drop-off on stress, a plateau region was observed for a wide range of strains. The Young's modulus for neat epoxy and polymer blends) was determined by a linear regression to the slope of the stress-strain curve in the initial linear elastic region and summarized in Figure 6 (inset table). The young's modulus for neat epoxy and polymer blends were comparable. The young's modulus for higher concentration TCE polymer blends was calculated as 1.6 Gpa, much lower than the neat epoxy. The neat epoxy had the higher yield stress than the other two polymer blends systems, revealing that the ability of epoxy system to resisting damage declined with the addition of TCE polymers or PVCi polymers. While, on the other side, it brings in advantages in the application of a crack sensor, because the polymer blends could be more sensitive and easier to deform under stress.
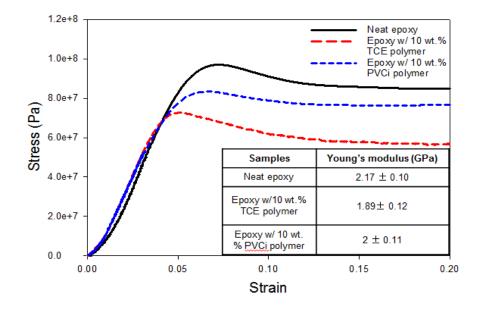
Figure 6. Compressive stress-strain curves for the pure epoxy and epoxy w/ 10 wt.% TCE polymers and PVCi polymers dispersed in the matrix. Inset table is the summary of Young's modulus of samples.

Fluorescence Response by Mechanical Activation

The goal for the application of cyclobutane-containing polymers in solid state here was to demonstrate mechanochemical cleavage of a covalent bond, and further to investigate the use of these cyclobutane-containing polymers blended with epoxy as stress/strain or damage sensors by visual detection. It is well-known that the force distribution is not uniform throughout a material under stress. The force distribution is dependent on the coupling between the macroscopic forces and the molecular forces. The spectroscopic signal can be measured and imaged to quantify the force.

Cracks were first generated by hammer smash on the neat epoxy and polymer blends. On neat epoxy, the cracks were observed under the white light only; there was nothing detected under the UV light, as displayed in Figure 7(a). Fluorescence emission along the cracks was clearly observed in Figure 7(b) under the UV light when epoxy was blended with 10 wt.% TCE

16

polymers, confirming that the fluorescence was due to the incorporation of TCE polymers. Cyclobutane is a four-membered ring molecule known for its highly strained structure, largely attributed to angle strain and torsional strain [51]. The mechanically induced cleavage of the C-C bonds of cyclobutane was thus relatively easy. It implied that, in the polymer blends, the cleavage of cyclobutane was the major reaction under stress since the C-C bond on cyclobutane was much weaker than the bonds in epoxy polymer structure. The corresponding images of epoxy with 20 wt.% and 30 wt.% TCE polymers are displayed in Figure 7(c) and (d). As images shown, the fluorescent signal was further augmented with increasing amount of TCE polymers blended with epoxy, implying that more mechanically induced reactions on cyclobutane occurred under stress. From the images, it's observed that epoxy with 10 wt.% TCE polymer gave sufficient fluorescent emission to detect the damage. Thus, the content of 10 wt.% was used for the following fluorescent tests.
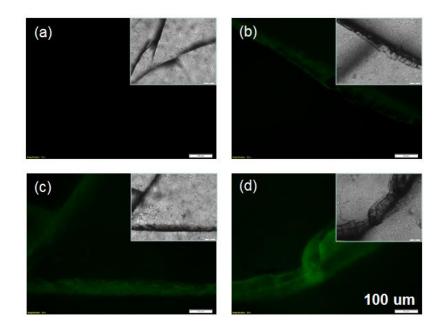

Figure 7. Microscopic images of fluorescence emission along cracks generated by hammer smash on polymer blends (a) without (b) with 10 wt.% (c) 20 wt.% (d) 30 wt.% TCE polymers. The insets were the corresponding images under white light.

In a compression test on epoxy with 10 wt.% TCE polymers, the fluorescent signal was monitored at six points on stress-strain curve, as shown in Figure 8(a). The evolution of induced fluorescence emission on the polymer blends is displayed through representative images at point a (right before the yield point), point b (right after the yield point) and point c (with strain of 20%). There was no obvious fluorescence observed before the yield point was reached; right after the yield point, the micro-cracks were observed under UV by fluorescence emission, while they were not observed under white light, indicating that the fluorescence emission could provide a higher sensitivity and easy detection for the location of cracks, especially for early damage detection, even though the initiation of crack formation usually goes unnoticed under the white light. It is also noticed that fluorescence emission along the crack intensified with strain after the yield point. The compression test was conducted on epoxy with 10 wt.% PVCi polymers. Both polymer blends displayed the similar behavior on fluorescent response under stress. The molecular architecture is very important for force transfer through bulk material to cleavable bond on mechanophore. TCE had three cinnamate functional groups on each molecule, the cycloaddition of cinnamates leaded to the formation of three-dimensional network; PVCi had multiple cinnamate functional groups as the chain side which connected the poly vinyl chain into a network through cyclobutane acting as a cross-linker. In the compression test, both polymer structures allowed for efficient transfer of mechanical force through bulk epoxy matrix to active mechanochemical reaction on cyclobutane, therefore inducing fluorescence generation. For comparison, tensile test was conducted on polymer blends. Polymer blends tested in tension failed in a brittle manner and no visual fluorescence was detected before the failure or at the fracture surface after the failure.
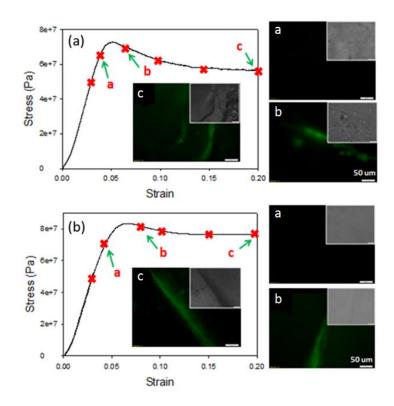
Figure 8. Microscopic images of fluorescence emission of (a) epoxy w/ 10 wt.% TCE polymers and (b) epoxy w/ 10 wt.% PVCi polymers at different strains.

In order to explore further the relationship between the strains and their corresponding fluorescence response, ten fluorescent micrographs at each point were processed by ImageJ. The integrated intensity was calculated through the sum of pixel values in image. The density at each point was averaged and plotted as a function of strain, as shown in Figure 9. Onset of activation was observed below 6% strain and 8% strain (just past the yield point) for epoxy with TCE polymers and epoxy with PVCi polymers, respectively. The density increased with the accumulation of strain, which indicated that the activation of cleavage of cyclobutane was achieved at low strain and more activations occurred with mechanical loading. Epoxy with 20 wt. % TCE polymers (Figure 9, top (inset)) displays the similar trend that is fluorescent intensity increases with strain.
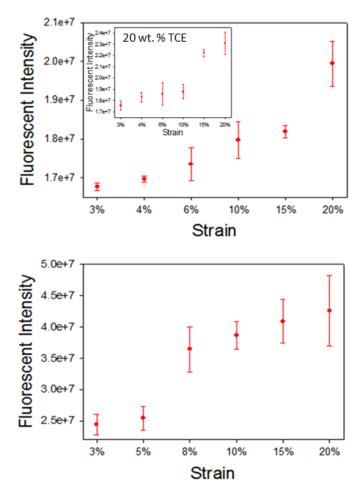
19

Figure 9. Integrated density of fluorescence emission in response to different strains of epoxy w/ 10 wt. % (top) TCE polymers (inset is 20% wt.% TCE) and (bottom) PVCi polymers.

4. CONCLUSION

We have studied the effect on the thermal properties and mechanical properties with the addition of cyclobutane-containing cross-linked polymer into an epoxy matrix. The cross-linked TCE and PVCi polymers were both thermally stable for a wide range of temperature. The DSC experiment showed that the addition of cross-linked TCE and PVCi polymer shifted the glass transition temperature (T_g) to lower temperatures, likely due to a lower cross-linking degree of epoxy. In the compression test, the emergence of cracks was detected by fluorescence at a strain level right beyond the yield point of the blended polymer system and the fluorescence intensified

with accumulation of strain. The fluorescence provided a higher sensibility for visual detection compared to observation by white light. Moreover, the possibilities of multiple stress sensors mechanically activated at different levels, which can be blended together as a more complex mechanophore combination will be an exciting undertaking.

5. ACKNOWLEDGEMENTS

REFERENCE

1.   Dasgupta, A.; Pecht, M. Material Failure Mechanisms and Damage Models. Ieee Transactions on Reliability 1991, 40, 531-536.

2.   Sih, G. C.; Tang, X. S. Micro/Macro-Crack Growth Due to Creep-Fatigue Dependency on Time-Temperature Material Behavior. Theoretical and Applied Fracture Mechanics 2008, 50, 9-22.

3.   Kwon, J. D.; Park, J. C.; Lee, Y. S.; Lee, W. H.; Park, Y. W. An Investigation of the Degradation Characteristics for Casting Stainless Steel, Cf8m, under High Temperatures. Nuclear Engineering and Design 2000, 198, 227-240.

4.   Drummond, J. L. Degradation, Fatigue, and Failure of Resin Dental Composite Materials. Journal of Dental Research 2008, 87, 710-719.

5.   John, R.; Jata, K. V.; Sadananda, K. Residual Stress Effects on near-Threshold Fatigue Crack Growth in Friction Stir Welds in Aerospace Alloys. International Journal of Fatigue 2003, 25, 939-948.

6.   Farrar, C. R.; Worden, K. An Introduction to Structural Health Monitoring. Philosophical Transactions of the Royal Society a-Mathematical Physical and Engineering Sciences 2007, 365, 303-315.

7.   Ortiz, M. Microcrack Coalescence and Macroscopic Crack-Growth Initiation in Brittle Solids. International Journal of Solids and Structures 1988, 24, 231-250.

8.   Ritchie, R. O. Mechanisms of Fatigue-Crack Propagation in Ductile and Brittle Solids. International Journal of Fracture 1999, 100, 55-83.

9.   Giurgiutiu, V.; Zagrai, A. Damage Detection in Thin Plates and Aerospace Structures with the Electro-Mechanical Impedance Method. Structural Health Monitoring-an International Journal 2005, 4, 99-118.

10.   Hamzeloo, S. R.; Shamshirsaz, M.; Rezaei, S. M. Damage Detection on Hollow Cylinders by Electro-Mechanical Impedance Method: Experiments and Finite Element Modeling. Comptes Rendus Mecanique 2012, 340, 668-677.

11.   Zagrai, A. N.; Giurgiutiu, V. Electro-Mechanical Impedance Method for Crack Detection in Thin Plates. Journal of Intelligent Material Systems and Structures 2001, 12, 709-718.

12.   Kessler, S. S.; Spearing, S. M.; Soutis, C. Damage Detection in Composite Materials Using Lamb Wave Methods. Smart Materials & Structures 2002, 11, 269-278.

13.   Monnier, T. Lamb Waves-Based Impact Damage Monitoring of a Stiffened Aircraft Panel Using Piezoelectric Transducers. Journal of Intelligent Material Systems and Structures 2006, 17, 411-421.

14.   Zhang, Y. In Piezoelectric Paint Sensor for Real-Time Structural Health Monitoring, 2005,1095-1103.

15.   Ali, R.; Mahapatra, D. R.; Gopalakrishnan, S. Constrained Piezoelectric Thin Film for Sensing of Subsurface Cracks. Smart Materials & Structures 2005, 14, 376-386.

16.   Rattanachan, S.; Miyashita, Y.; Mutoh, Y. Fabrication of Piezoelectric Laminate for Smart Material and Crack Sensing Capability. Science and Technology of Advanced Materials 2005, 6, 704-711.

17.   Pucci, A.; Di Cuia, F.; Signori, F.; Ruggeri, G. Bis(Benzoxazolyl)Stilbene Excimers as Temperature and Deformation Sensors for Biodegradable Poly(1,4-Butylene Succinate) Films. Journal of Materials Chemistry 2007, 17, 783-790.

18.   Chi, Z. G.; Zhang, X. Q.; Xu, B. J.; Zhou, X.; Ma, C. P.; Zhang, Y.; Liu, S. W.; Xu, J. R. Recent Advances in Organic Mechanofluorochromic Materials. Chemical Society Reviews 2012, 41 (10), 3878-3896.

19.   Crenshaw, B. R.; Burnworth, M.; Khariwala, D.; Hiltner, A.; Mather, P. T.; Simha, R.; Weder, C. Deformation-Induced Color Changes in Mechanochromic Polyethylene Blends. Macromolecules 2007, 40, 2400-2408.

20.   Chen, Y. L.; Spiering, A. J. H.; Karthikeyan, S.; Peters, G. W. M.; Meijer, E. W.; Sijbesma, R. P. Mechanically Induced Chemiluminescence from Polymers Incorporating a 1,2-Dioxetane Unit in the Main Chain. Nature Chemistry 2012, 4, 559-562.

21.   Neebe, M.; Rhinow, D.; Schromczyk, N.; Hampp, N. A. Thermochromism of Bacteriorhodopsin and Its Ph Dependence. Journal of Physical Chemistry B 2008, 112, 6946-6951.

22.   Durr, H. A New Photochromic System - Potential Limitations and Perspectives. Pure and Applied Chemistry 1990, 62, 1477-1482.

23.   Schonberg, A.; Elkaschef, M.; Nosseir, M.; Sidky, M. M. Experiments with 4-Thiopyrones and with 2,2',6,6'-Tetraphenyl-4,4'-Dipyrylene - the Piezochromism of Diflavylene. Journal of the American Chemical Society 1958, 80, 6312-6315.

24.   Yoshida, M.; Nakanishi, F.; Seki, T.; Sakamoto, K.; Sakurai, H. Two-Dimensional Piezochromism and Orientational Modulations in Polysilane Monolayer. Macromolecules 1997, 30, 1860-1862.

25.   Davis, D. A.; Hamilton, A.; Yang, J. L.; Cremar, L. D.; Van Gough, D.; Potisek, S. L.; Ong, M. T.; Braun, P. V.; Martinez, T. J.; White, S. R.; Moore, J. S.; Sottos, N. R. Force-Induced Activation of Covalent Bonds in Mechanoresponsive Polymeric Materials. Nature 2009, 459, 68-72.

26.   Cho, S. Y.; Kim, J. G.; Chung, C. M. Photochemical Crack Healing in Cinnamate-Based Polymers. Journal of Nanoscience and Nanotechnology 2010, 10, 6972-6976.

27.   Bucknall, C. B.; Gilbert, A. H. Toughening Tetrafunctional Epoxy-Resins Using Polyetherimide. Polymer 1989, 30, 213-217.

28.   Cantwell, W. J.; Morton, J. The Impact Resistance of Composite-Materials - a Review. Composites 1991, 22, 347-362.

29.   Allaoui, A.; Bai, S.; Cheng, H. M.; Bai, J. B. Mechanical and Electrical Properties of a Mwnt/Epoxy Composite. Composites Science and Technology 2002, 62, 1993-1998.

30.   Bascom, W. D.; Cottington, R. L.; Jones, R. L.; Peyser, P. Fracture of Epoxy-Modified and Elastomer-Modified Epoxy Polymers in Bulk and as Adhesives. Journal of Applied Polymer Science 1975, 19, 2545-2562.

31.   Cho, S. Y.; Kim, J. G.; Chung, C. M. A Fluorescent Crack Sensor Based on Cyclobutane-Containing Crosslinked Polymers of Tricinnamates. Sensors and Actuators B-Chemical 2008, 134, 822-825.

32.   Oya, N.; Sukarsaatmadja, P.; Ishida, K.; Yoshie, N. Photoinduced Mendable Network Polymer from Poly(Butylene Adipate) End-Functionalized with Cinnamoyl Groups. Polymer Journal 2012, 44, 724-729.

33.   Ali, A. H.; Srinivasan, K. S. V, Photoresponsive Functionalized Vinyl Cinnamate Polymers: Synthesis and Characterization. Polymer International 1997, 43, 310-316.

34.   Iimura, Y.; Kobayashi, S.; Hashimoto, T.; Sugiyama, T.; Katoh, K. Alignment Control of Liquid Crystal Molecules Using Photo-Dimerization Reaction of Poly(Vinyl Cinnamate). Ieice Transactions on Electronics 1996, E79C, 1040-1046.

35.   Murase, S.; Kinoshita, K.; Horie, K.; Morino, S. Photo-Optical Control with Large Refractive Index Changes by Photodimerization of Poly(Vinyl Cinnamate) Film. Macromolecules 1997, 30, 8088-8090.

36.   Tsuda, M. Some Aspects of Photosensitivity of Poly(Vinyl Cinnamate). Journal of Polymer Science Part a-General Papers 1964, 2, 2907-&.

37.   Kim, T. D.; Bae, H. M.; Lee, K. S. Synthesis and Characterization of a New Polyester Having Photo-Crosslinkable Cinnamoyl Group. Bulletin of the Korean Chemical Society 2002, 23, 1031-1034.

38.   Coleman, M. M.; Hu, Y.; Sobkowiak, M.; Painter, P. C. Infrared Characterization of Poly(Vinyl Cinnamate) and Its Blends with Poly(4-Vinyl Phenol) before and after Uv Exposure. Journal of Polymer Science Part B-Polymer Physics 1998, 36, 1579-1590.

39.   Chae, B.; Lee, S. W.; Ree, M.; Jung, Y. M.; Kim, S. B. Photoreaction and Molecular Reorientation in a Nanoscaled Film of Poly(Methyl 4-(Methacryloyloxy)Cinnamate) Studied by Two-Dimensional Ftir and Uv Correlation Spectroscopy. Langmuir 2003, 19, 687-695.

40.   Brostow, W.; Chiu, R.; Kalogeras, I. M.; Vassilikou-Dova, A. Prediction of Glass Transition Temperatures: Binary Blends and Copolymers. Materials Letters 2008, 62, 3152-3155.

41.   Zhou, J. M.; Lucas, J. P. Hygrothermal Effects of Epoxy Resin. Part Ii: Variations of Glass Transition Temperature. Polymer 1999, 40, 5513-5522.

42.   Rebizant, V.; Venet, A. S.; Tournilhac, F.; Girard-Reydet, E.; Navarro, C.; Pascault, J. P.; Leibler, L. Chemistry and Mechanical Properties of Epoxy-Based Thermosets Reinforced by Reactive and Nonreactive Sbmx Block Copolymers. Macromolecules 2004, 37, 8017-8027.

43.   Sun, Y. Y.; Zhang, Z. Q.; Moon, K. S.; Wong, C. P. Glass Transition and Relaxation Behavior of Epoxy Nanocomposites. Journal of Polymer Science Part B-Polymer Physics 2004, 42, 3849-3858.

44.   Bandyopadhyay, A.; Valavala, P. K.; Clancy, T. C.; Wise, K. E.; Odegard, G. M. Molecular Modeling of Crosslinked Epoxy Polymers: The Effect of Crosslink Density on Thermomechanical Properties. Polymer 2011, 52, 2445-2452.

45.   Blumstei.A. Polymerization of Adsorbed Monolayers .2. Thermal Degradation of Inserted Polymer. Journal of Polymer Science Part a-General Papers 1965, 3, 2665-&.

46.   Collier, A.; Wang, H. J.; Yuan, X. Z.; Zhang, J. J.; Wilkinson, D. P. Degradation of Polymer Electrolyte Membranes. International Journal of Hydrogen Energy 2006, 31, 1838-1854.

47.   Chattopadhyay, D. K.; Webster, D. C. Thermal Stability and Flame Retardancy of Polyurethanes. Progress in Polymer Science 2009, 34, 1068-1133.

48.   Aoyagi, Y.; Yamashita, K.; Doi, Y. Thermal Degradation of Poly (R)-3-Hydroxybutyrate , Poly Epsilon-Caprolactone , and Poly (S)-Lactide. Polymer Degradation and Stability 2002, 76 (1), 53-59.

49.   Starnes, W. H. Structural and Mechanistic Aspects of the Thermal Degradation of Poly(Vinyl Chloride). Progress in Polymer Science 2002, 27, 2133-2170.

50.   Kim, H. T.; Park, J. K. Thermal Degradation of Poly(Vinyl Cinnamate). Polymer Bulletin 1998, 41, 325-331.

51.   Bach, R. D.; Dmitrenko, O. Strain Energy of Small Ring Hydrocarbons. Influence of C-H Bond Dissociation Energies. Journal of the American Chemical Society 2004, 126, 4444-4452.